J Membrane Biol (2013) 246:893–902
DOI 10.1007/s00232-013-9589-9

Divalent Cations Modulate TMEM16A Calcium-Activated Chloride Channels by a Common Mechanism

Hongbo Yuan · Chongsen Gao · Yafei Chen · Mengwen Jia · Jinpeng Geng · Hailin Zhang · Yong Zhan · Linda M. Boland · Hailong An

Received: 21 February 2013 / Accepted: 9 August 2013 / Published online: 31 August 2013

Abstract The gating of Ca^{2+}-activated Cl^- channels is controlled by a complex interplay among $[Ca^{2+}]_i$, membrane potential and permeant anions. Besides Ca^{2+}, Ba^{2+} also can activate both TMEM16A and TMEM16B. This study reports the effects of several divalent cations as regulators of TMEM16A channels stably expressed in HEK293T cells. Among the divalent cations that activate TMEM16A, Ca^{2+} is most effective, followed by Sr^{2+} and Ni^{2+}, which have similar affinity, while Mg^{2+} is ineffective. Zn^{2+} does not activate TMEM16A but inhibits the Ca^{2+}-activated chloride currents. Maximally effective concentrations of Sr^{2+} and Ni^{2+} occluded activation of the TMEM16A current by Ca^{2+}, which suggests that Ca^{2+}, Sr^{2+} and Ni^{2+} all regulate the channel by the same mechanism.

Electronic supplementary material The online version of this article (doi:10.1007/s00232-013-9589-9) contains supplementary material, which is available to authorized users.

H. Yuan · C. Gao · Y. Chen · M. Jia · J. Geng · Y. Zhan (✉) · H. An (✉)
Institute of Biophysics, School of Sciences, Hebei University of Technology, 5340 Xiping Road, Tianjin 300401, People's Republic of China
e-mail: zhany@hebut.edu.cn

H. An
e-mail: hailong_an@hebut.edu.cn

H. Zhang
Key Laboratory of Neural and Vascular Biology, Ministry of Education, The Key Laboratory of Pharmacology and Toxicology for New Drug, Hebei Province, Department of Pharmacology, Hebei Medical University, Shijiazhuang 050017, People's Republic of China

L. M. Boland (✉)
Department of Biology, University of Richmond, Richmond, VA 23114, USA
e-mail: lboland@richmond.edu

Keywords TMEM16A · Divalent cation · Regulation · Patch clamp

Abbreviaitions

CaCCs	Ca^{2+}-activated Cl^- currents
$[Ca^{2+}]_i$	Intracellular calcium concentration
V_m	Membrane potential

Introduction

Ca^{2+}-activated Cl^- currents (CaCCs) were first discovered about 30 years ago in *Xenopus* oocytes (Barish 1983; Miledi 1982) and salamander photoreceptor inner segments (Bader et al. 1982). In the oocytes, CaCCs play a role in the blockade of sperm penetration once an initial fertilization has occurred, thus preventing polyspermy (Hartzell et al. 2005). In vertebrate photoreceptors, CaCCs play a role in neurotransmitter release (MacLeish and Nurse 2007). In addition to these examples, CaCCs have since been implicated in many physiological functions including epithelial fluid secretion, olfactory transduction, vascular smooth muscle contraction, taste adaptation, cell volume regulation and the regulation of neuronal and cardiac excitability (Huang et al. 2012). Changes in the expression or function of CaCCs may also play a role in cancer cell proliferation (Huang et al. 2009), enhancing the importance of understanding the mechanisms of CaCCs function.

The activation of CaCCs/TMEM16A by Ca^{2+} exhibits a unique voltage dependence, which may be explained by the presence of a calcium binding site with the membrane electric field (Hartzell et al. 2005). At low internal Ca^{2+} concentrations, the current–voltage relationship for CaCCs/TMEM16A is outwardly rectifying. However, at high

internal Ca^{2+} concentrations, the channels are activated fully at all membrane potentials and the current–voltage relationship becomes linear (Caputo et al. 2008; Schroeder et al. 2008; Young et al. 2008). A structural basis for the activation of CaCCs/TMEM16A by Ca^{2+} ions remains incompletely understood and might be improved by studying a broader range of divalent cations.

Recently, two members of the TMEM16 family (TMEM16A and TMEM16B, also known as ANO1 and ANO2) were identified as the molecular correlates of CaCCs. TMEM16A and TMEM16B are dually gated by membrane voltage (V_m) and intracellular Ca^{2+}, like their native counterparts. Indeed, the Ca^{2+} affinities of both TMEM16A and TMEM16B are voltage-dependent, and the pharmacological profiles match those found for the *Xenopus* oocyte CaCCs (Schroeder et al. 2008). What is more, both Ca^{2+} and other divalent cations have activation effects. TMEM16A can be activated by Ba^{2+} (Xiao et al. 2011), and Stephan et al. (2009) have shown that Sr^{2+} and Ba^{2+} can activate TMEM16B but Ba^{2+} has a weaker effect. However, the cloning of TMEM16A and TMEM16B has not yet revealed a crystal structural explanation for the Ca^{2+}-dependent regulation of CaCCs. Neither protein possesses an EF hand-like Ca^{2+}-binding site or an IQ-domain calmodulin binding site (Huang et al. 2012). Xiao et al. (2011) found that deleting $_{448}EAVK_{451}$ in the first intracellular loop dramatically decreases apparent Ca^{2+} affinity. In contrast, mutating the adjacent amino acids $_{444}EEEE_{447}$ abolishes intrinsic voltage dependence without altering the apparent Ca^{2+} affinity (Xiao et al. 2011). Similarly, E_{367} and $_{386}EEEEE_{390}$ in the first intracellular putative loop play an important role in the voltage dependence of TMEM16B (Cenedese et al. 2012). Moreover, E_{702} and E_{705} in the third intracellular Loop contribute to Ca^{2+} gating (Yu et al. 2012), and I317A and I762A mutants influence the combination of ANO1 and CaM (Jung et al. 2013). A more thorough investigation of divalent cation regulation of TMEM channels could help address the structural basis for the chloride channel's function and lay a foundation for understanding how divalent cations regulate other ion channels.

In this article, we examine the divalent cation regulation of TMEM16A in a stably transfected HEK293T cell line which we established. We present the first characterization of the divalent cation dependence of the TMEM16A chloride currents using whole-cell and excised patch recordings. We show that intracellular Ca^{2+}, Sr^{2+} and Ni^{2+} activate TMEM16A, whereas Mg^{2+} do not activate this channel. Zn^{2+} also fails to

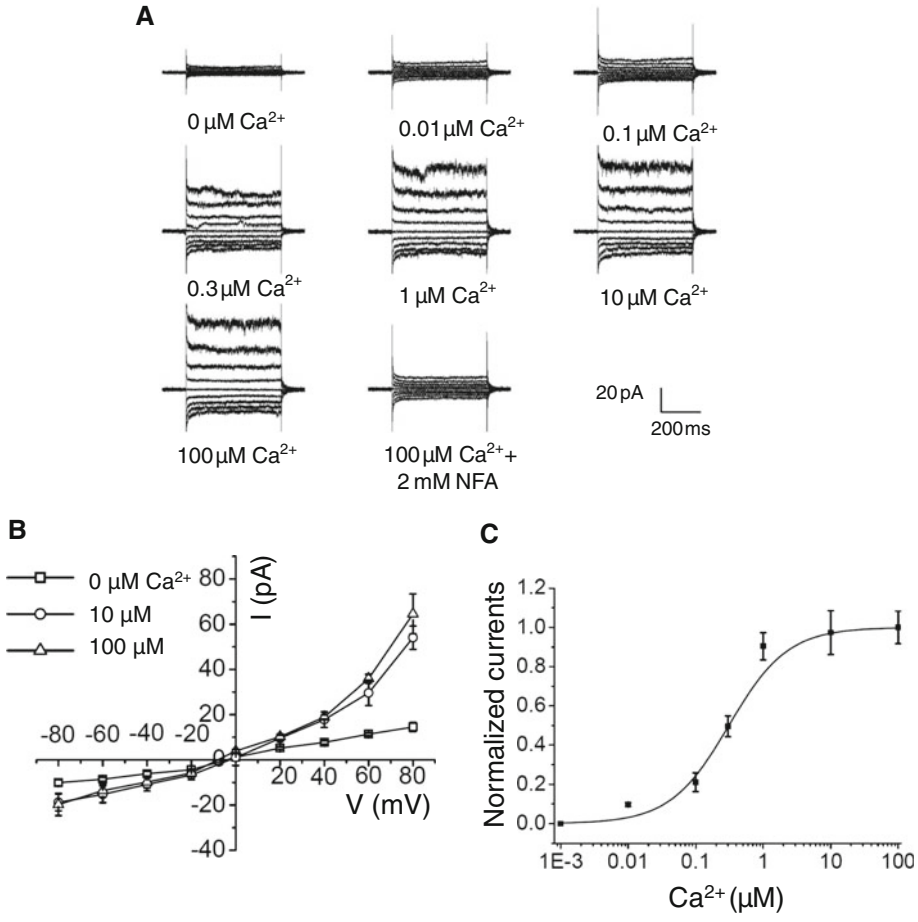

Fig. 1 Ca^{2+} and voltage dependence of TMEM16A chloride current activation in stably transfected HEK293T cells. **a** Representative current families elicited by increasing concentrations of Ca^{2+} applied to the intracellular surface of inside-out membrane patches. Currents were recorded at step potentials from −80 to +80 mV in +20-mV increments from a holding potential of 0 mV. **b** Current–voltage relationships for 0, 10 and 100 Ca^{2+}, measured as in **a** ($n = 4$). **c** A concentration–response relationship for TMEM16A activation by intracellular Ca^{2+}. Current magnitudes were normalized to those measured at 1 mM Ca^{2+} and +80 mV in each patch. Data points were fitted to the Hill equation with n_H (slope) = 1.3 and $EC_{50} = 309.73 \pm 37.53$ nM. *Error bars*, mean ± SEM, $n = 4$

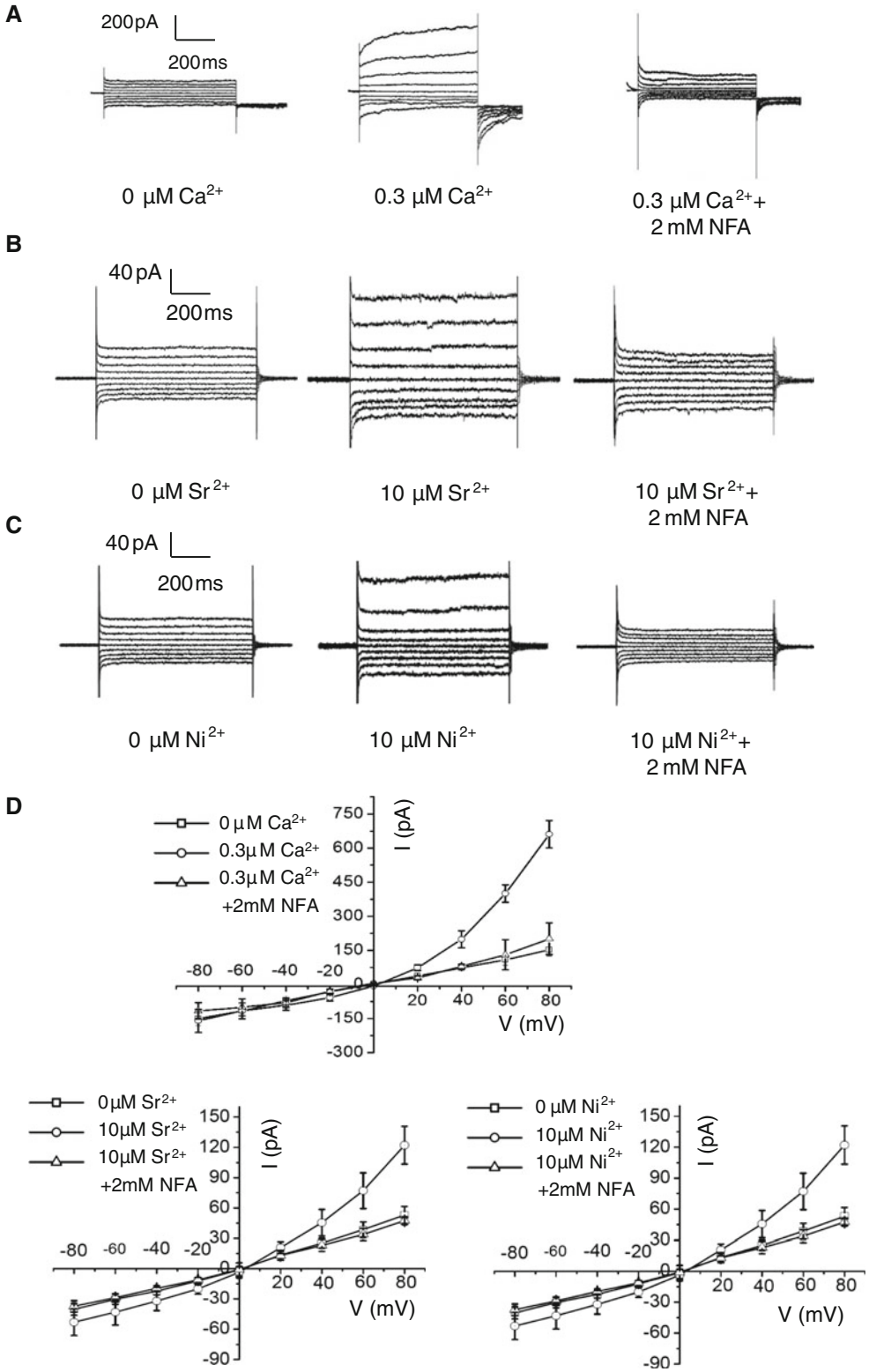

Fig. 2 Ca^{2+}, Sr^{2+} and Ni^{2+} activate TMEM16A from the intracellular side. Representative whole-cell currents activated by intracellular **a** Ca^{2+}, **b** Sr^{2+} and **c** Ni^{2+} with the divalent cation applied in the pipette solution. Niflumic acid (*NFA*, 2 mM) was applied in the bath to patches recorded in EC_{50} (Ca^{2+} = 0.3 μM, Sr^{2+}=10 μM, Ni^{2+} = 10 μM) divalent cation. Currents were recorded at step potentials from −80 to +80 mV in +20-mV increments from a holding potential of 0 mV. **d** Current–voltage relationships for 0 μM and EC_{50} Ca^{2+}, Sr^{2+} or Ni^{2+} as well as EC_{50} divalent plus 2 mM NFA (n = 6)

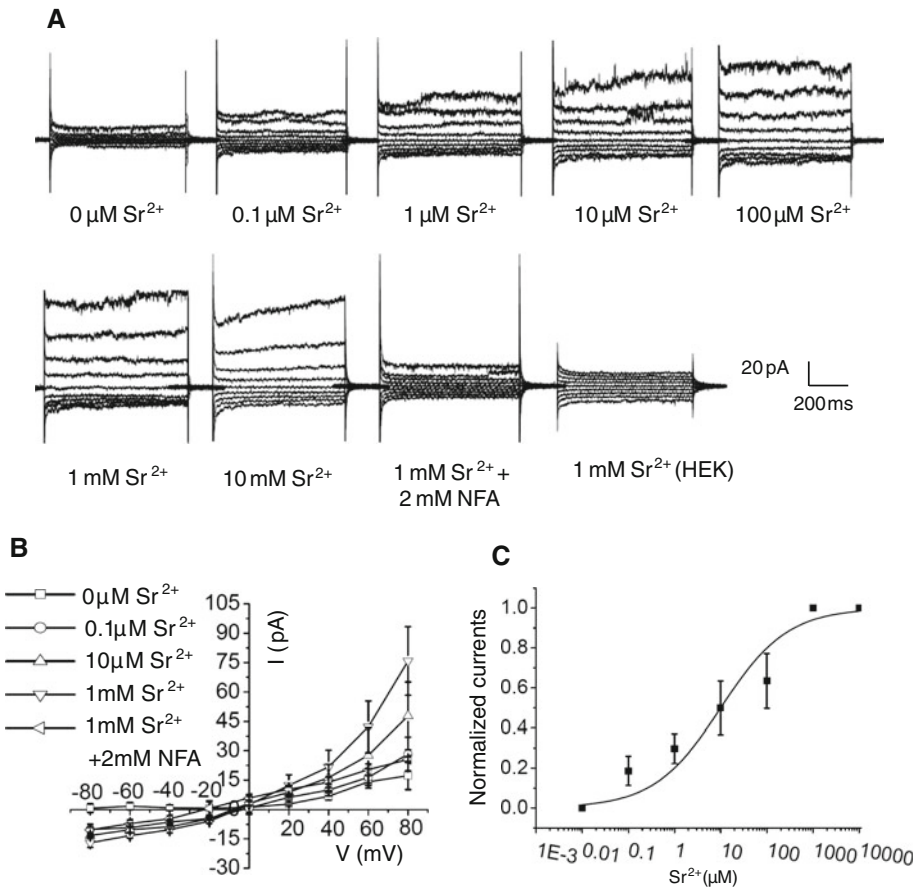

Fig. 3 Concentration dependence of Sr^{2+} activation of TMEM16A. **a** Representative current families elicited by increasing concentrations of Sr^{2+} applied to the intracellular surface of inside-out membrane patches. Currents were recorded at step potentials from −80 to +80 mV in +20-mV increments from a holding potential of 0 mV. The last panel of current traces in **a** is from 1 mM Sr^{2+} applied to a membrane patch from an untransfected HEK cell. **b** Current–voltage relationships for 0, 10 and 100 Sr^{2+}, measured as in **a** ($n = 7$). **c** A concentration–response relationship for TMEM16A activation by intracellular Sr^{2+}. Current magnitudes were normalized to those measured at 1 mM Sr^{2+} and +80 mV in each patch. Data points were fitted to the Hill equation with n_H (slope) = 0.6 and $EC_{50} = 9.99 \pm 0.25$ μM. *Error bars*, mean ± SEM, $n = 7$

activate TMEM16A, although it blocks the TMEM16A currents activated by intracellular Ca^{2+}. These findings add to our knowledge of the impact of divalent cations on an important class of chloride channels and may shed light on understanding the gating of TMEM16A/CaCCs.

Materials and Methods

Chemicals

All cell culture reagents and Lipofectamine 2000 were purchased from Invitrogen (Carlsbad, CA, USA). HEPES, $MgCl_2 \cdot 6H_2O$, niflumic acid (NFA), EGTA, gluconate sodium salt and $CaCl_2$ solution were purchased from Sigma-Aldrich (Shanghai, China). Other chemical reagents were purchased from Biodee (Beijing, China).

Cell Culture and Stable Transfection

The human cDNA clone hANO1, also called TMEM16A (accession NM_178642.5), was kindly provided by Prof. Young Duk Yang (Seoul National University, Korea) and subcloned to expression vector pEGFPN1 (Clontech, Mountain View, CA, USA). HEK293T cells were maintained in DMEM with 10 % fetal bovine serum, 100 UI/ml penicillin and 100 μg/ml streptomycin and passaged about three times a week. Stable transfection of pETMEM16A into HEK293T cells was performed as described by Jia et al. (2007) with Lipofectamine 2000. Stably transfected HEK293T cells were seeded in 24-well plates on 12-mm glass coverslips, 1 day before patch recording. All cells were maintained in an incubator with 5 % CO_2, 37 °C.

Solutions

For whole-cell recording, the pipette solution contained (in mM) 130 CsCl, 10 EGTA, 1 $MgCl_2$, 10 HEPES, adjusted to pH 7.3 with CsOH. $CaCl_2$, $SrCl_2$, $NiCl_2$ and $ZnCl_2$, diluted from 1 M stock solutions were added to the pipette solution to obtain various free concentrations of divalent cations, as determined with the Ca-EGTA calculator (http://www.stanford.edu/~cpatton/CaEGTA-NIST.htm). The bath perfusion solution contained (in mM) 150 NaCl, 5 EGTA, 1 $MgCl_2$ and 10 HEPES, adjusted to pH 7.4 with NaOH.

For inside-out patch recordings, we used symmetrical solutions. Both the pipette and perfusion solutions contained (in mM) 130 NaCl, 1 $MgCl_2 \cdot 6H_2O$, 10 HEPES and 1 MgATP, adjusted to pH 7.3 with CsOH. Divalent cations were added to calculated concentrations, as described for

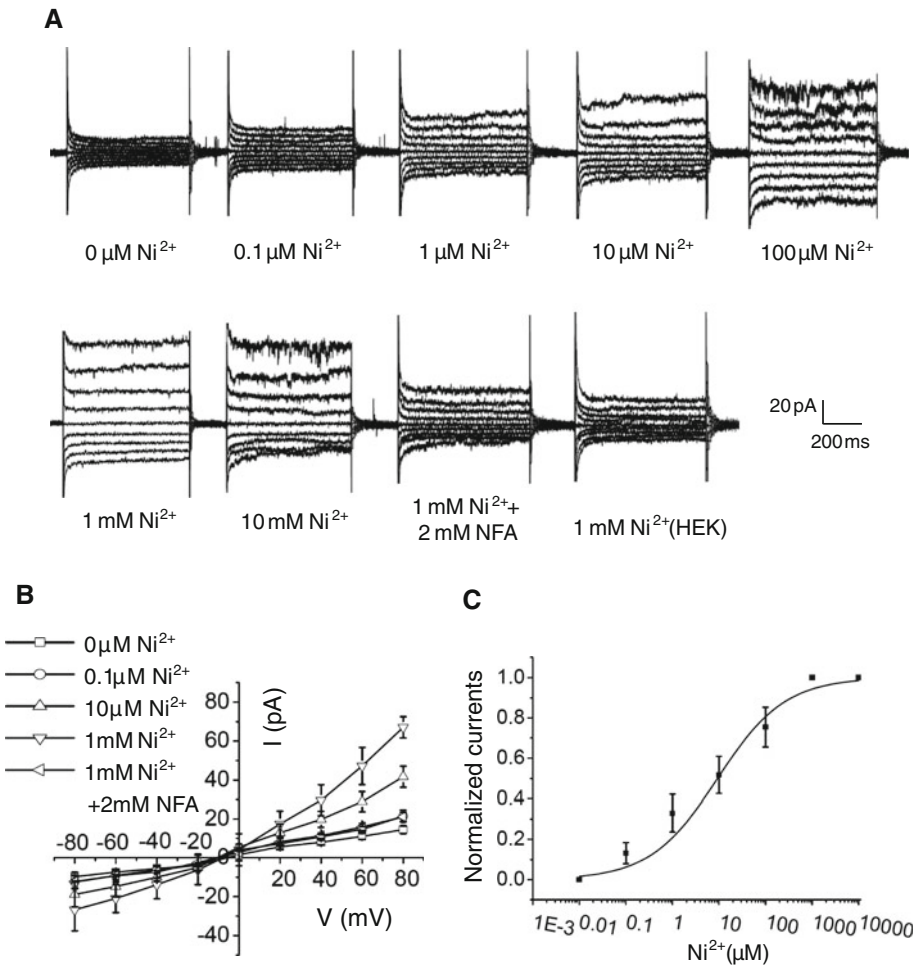

Fig. 4 Concentration dependence of Ni^{2+} activation of TMEM16A. **a** Representative current families elicited by increasing concentrations of Ni^{2+} applied to the intracellular surface of inside-out membrane patches. Currents were recorded at step potentials from −80 to +80 mV in +20-mV increments from a holding potential of 0 mV. The last *panel* of current traces in **a** is from 1 mM Ni^{2+} applied to a membrane patch from an untransfected HEK cell. **b** Current–voltage relationships for 0, 10 and 100 Ni^{2+}, measured as in **a** ($n = 6$). **c** A concentration–response relationship for TMEM16A activation by intracellular Ni^{2+}. Current magnitudes were normalized to those measured at 1 mM Ni^{2+} and +80 mV in each patch. Data points were fitted to the Hill equation with n_H (slope) = 0.6 and $EC_{50} = 9.32 \pm 0.33$ μM. *Error bars*, mean ± SEM, $n = 6$

whole-cell recordings. NFA was dissolved in dimethyl sulfoxide as a 100-mM stock solution and diluted to 2 mM in the bath perfusion solution for inside-out recordings.

Electrophysiology

Electrophysiological recordings from HEK293T cells stably transfected with TMEM16A were performed in whole-cell or inside-out patch clamp configurations. Patch pipettes were made of borosilicate glass (VitalSense, Wuhan, China) with a P-97 puller (Sutter Instruments, Novato, CA, USA) and fire-polished to resistances of 600–800 KΩ (inside-out) or 2–4 MΩ (whole-cell). Different bathing solutions were delivered using a gravity-fed perfusion system. A complete solution change was obtained in about 2 min.

Data acquisition was performed with an EPC-10 amplifier controlled by Pulse software with Digi LIH1600 interface (HEKA, Lambrecht/Pfalz, Germany). Data were low pass–filtered at 2.9 kHz and sampled at 3.33 kHz. All measurements were performed at room temperature. Graphics and statistical data analysis were carried out with Origin 8.0 (OriginLab, Northampton, MA, USA).

Results

Expression of TMEM16A in Stably Transfected HEK293T Cells

To study the electrophysiological properties of TMEM16A in mammalian cells, we established stably transfected HEK293T cells and performed whole-cell and inside-out patch-clamp recordings with different bath solutions designed to measure the chloride currents. Our data show that the gating of TMEM16A in stably transfected HEK cells has voltage and Ca^{2+} dependence (Fig. 1a), as previously recognized for expression of this chloride channel in HEK cell lines (Ferrera et al. 2009; Xiao et al. 2011). In Ca^{2+}-free solutions, there is no noticeable current. However, 10 μM Ca^{2+} activates NFA-sensitive chloride currents that are four- to fivefold larger than the endogenous currents in untransfected cells. The current–voltage relationship is nonlinear with increasing Ca^{2+} concentrations applied to the intracellular surface of excised patches (Fig. 1b). The EC_{50} for calcium activation of TMEM16A was determined from a fit of the concentration–response

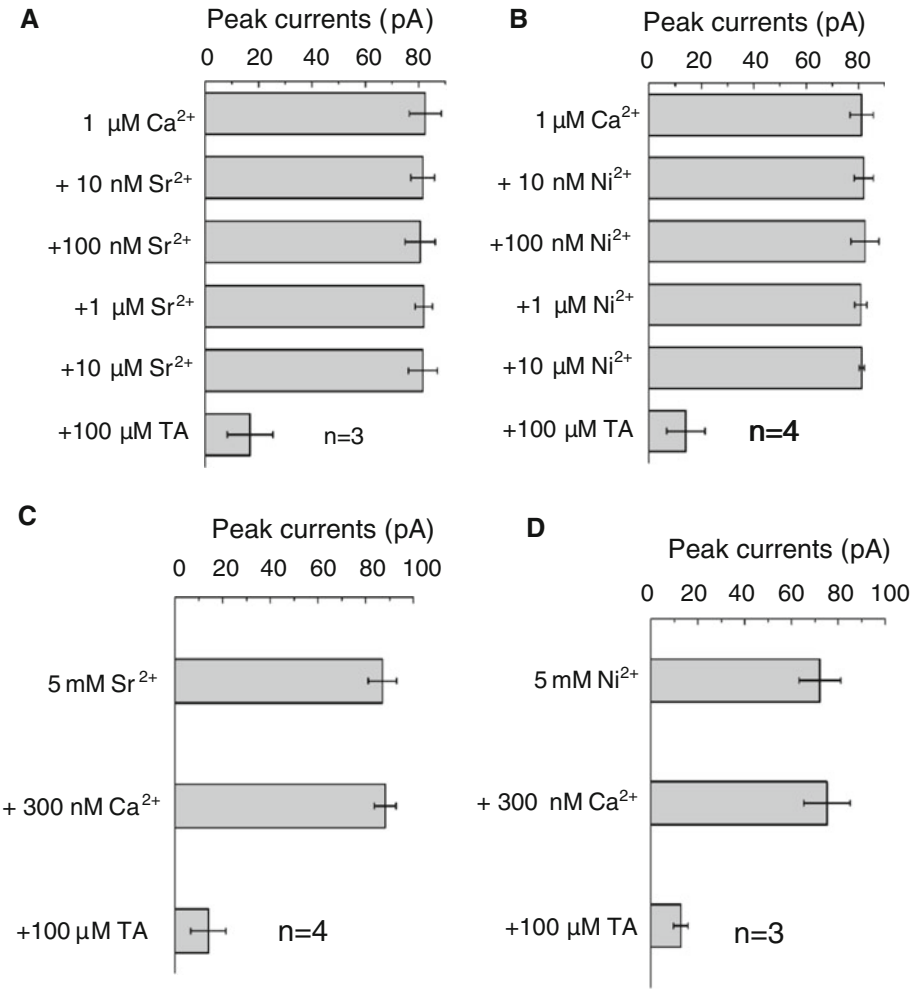

Fig. 5 Test for additivity of Sr^{2+}, Ni^{2+} and Ca^{2+} activation of TMEM16A. **a** Peak currents of TMEM16A activated by a gradient of Sr^{2+} concentrations, coapplied with 1 μM Ca^{2+}. **b** Peak currents of TMEM16A activated by a gradient of Ni^{2+} concentrations, coapplied with 1 μM Ca^{2+}. **c** Peak currents of TMEM16A activated by 5 mM Sr^{2+} alone and with 300 nM Ca^{2+}. **d** Peak currents of TMEM16A activated by 5 mM Ni^{2+} alone and with 300 nM Ca^{2+}. In each experiment, the chloride channel blocker tannic acid (TA) was used to confirm the nature of the ionic currents. All ionic solutions were applied to the internal surface of the membrane in inside-out patch recordings. Current amplitudes were measured at +80 mV

data to the Hill equation; the EC_{50} was 309.73 ± 37.53 nM at +80 mV, and 10 μM Ca^{2+} is a saturating concentration for TMEM16A current activation (Fig. 1c). Our data illustrate that the stably transfected TMEM16A also conserves the calcium dependence of CaCCs activation.

Sr^{2+} and Ni^{2+} Independently Activate TMEM16A

We tested the specificity of calcium as an activator of TMEM16A by examining current activation with other divalent cations. Independently, Sr^{2+} or Ni^{2+} induced whole-cell voltage-dependent chloride currents that were blocked by 2 mM NFA (Fig. 2a, b), a known blocker of chloride channels (Hartzell et al. 2005). As a negative control, we performed the same experiments on untransfected HEK293T cells and found that 1 mM Sr^{2+} or Ni^{2+} failed to induce currents in untransfected cells (Figs. 3a, 4a). Thus, the divalent cation–activated currents in the stably transfected cells were attributed to TMEM16A channels.

We determined the concentration–response relationship for current activation by Sr^{2+} or Ni^{2+} ions using inside-out patch-clamp recordings with the divalent cations applied to the intracellular surface of the membrane (Fig. 3a, b). The fitted EC_{50} values for current activation by Sr^{2+} and Ni^{2+} ions were 9.99 ± 0.25 and 9.32 ± 0.33 μM at +80 mV, respectively (Figs. 3c, 4c), about 30-fold higher than the EC_{50} for activation by Ca^{2+}. Likewise, a 1-mM concentration of Sr^{2+} or Ni^{2+} was a saturating concentration (Figs. 3c, 4c). These results show that Sr^{2+} or Ni^{2+} can mimic the effect of Ca^{2+} in the activation of TMEM16A. We also tested if Mg^{2+} can activate TMEM16A; however, up to 1 mM Mg^{2+} is inefficient to activate TMEM16A (data not shown).

Sr^{2+}, Ni^{2+} and Ca^{2+} Activate TMEM16A by a Common Mechanism

We used occlusion experiments to test the hypothesis that Sr^{2+}, Ni^{2+} and Ca^{2+} activate TMEM16A by a common mechanism. Increasingly higher concentrations of Sr^{2+} or Ni^{2+} (Fig. 5) were coapplied with a concentration of 1 μM Ca^{2+} ions in the bath solution in inside-out patch recordings. The TMEM16A currents were not enhanced by Sr^{2+} or Ni^{2+} (up to 10 μM) when compared to 1 μM Ca^{2+} alone

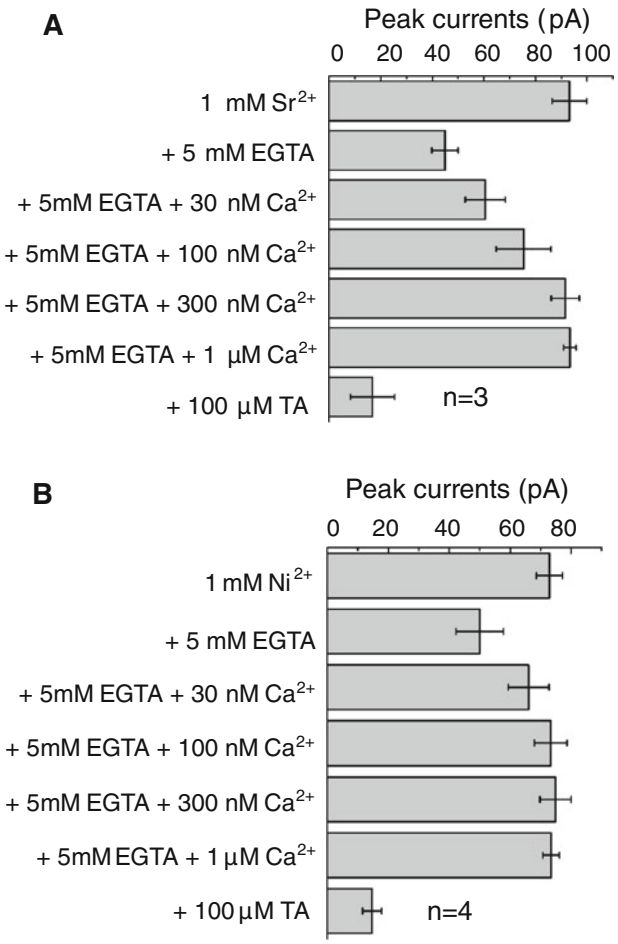

Fig. 6 Ca^{2+} recovers the chloride current after chelation of activating concentrations of Sr^{2+} or Ni^{2+}. Concentration-dependent recovery of the TMEM16A chloride currents by Ca^{2+} applications after EGTA-mediated chelation of high (5 mM) concentrations of Sr^{2+} (**a**) or Ni^{2+} (**b**). All ionic solutions were applied to the internal surface of the membrane in inside-out patch recordings. Current amplitudes were measured at +80 mV. Currents were blocked by tannic acid (TA) at the end of the experiment

(Fig. 5a, b). The measured currents were 90 % inhibited by 100 µM tannic acid (Figs. 5, 6), a specific blocker of CaCCs (Namkung et al. 2010). We also tested for additivity of activation by adding 300 nM Ca^{2+} to saturating concentrations (5 mM) of Sr^{2+} or Ni^{2+}; this failed to show an increase in the measured current (Fig. 5c, d). However, the currents activated by 1 mM Sr^{2+} or Ni^{2+} were reduced by up to 50 % in the presence of 5 mM of the divalent chelator EGTA and then recovered to maximal levels as the concentration of Ca^{2+} ions in the solution was increased to 1 µM (Fig. 6a, b), suggesting that Ca^{2+} could restore the current that had been previously activated by Sr^{2+} or Ni^{2+}. Thus, Sr^{2+}, Ni^{2+} and Ca^{2+} activate chloride currents in the TMEM16A cell line in a nonadditive fashion.

Zn^{2+} Ions Block TMEM16A Currents

In the stably transfected cells, there were no apparent CaCCs activated by Zn^{2+} up to a concentration of 10 µM (Supplementary Fig. 1), even though this concentration is greater than or equal to the EC_{50} for each of the three activating divalents. However, external application of Zn^{2+} blocked the whole-cell TMEM16A current that was activated by 1 µM Ca^{2+} in the pipette solution (Supplementary Fig. 2). We also determined the concentration dependence of Zn^{2+} block of CaCCs in inside-out patch recordings (Fig. 7); the IC_{50} was determined to be 12.85 ± 0.28 µM at +80 mV. As a negative control, we performed the same experiments on untransfected HEK cells and observed a failure to activate a chloride current by Ca^{2+} or Zn^{2+} alone or by the combined application of Ca^{2+} and Zn^{2+} (Supplementary Fig. 3). Thus, Zn^{2+} blocks the currents activated by calcium, but Zn^{2+} is not itself an activator of CaCCs.

Discussion

The gating of TMEM16A is controlled by a complex interplay among $[Ca^{2+}]_i$, V_m and permeant anions. Although for TMEM16A, Ca^{2+}- and voltage-dependent gating are very closely coupled, Xiao et al. (2011) showed that high concentrations of intracellular Ca^{2+} alone induce channel openings even at very hyperpolarized potentials. Therefore, there may exist more than one Ca^{2+}-binding domain. In recent years, some key amino acid residues or fragments involved in Ca^{2+} sensitivity of TMEM16A have been identified (Scudieri et al. 2013; Xiao et al. 2011; Yu et al. 2012). Calmodulin (CaM), a calcium-binding protein, can be modulated by both Ca^{2+} and other divalent cations, but Ca^{2+} is the most powerful activator (Chao et al. 1984). The reason is that the free energy of hydration of Ba^{2+} is smaller than that of Ca^{2+}; therefore, Ba^{2+} binding is less stable than that of Ca^{2+} (Falke et al. 1994). The EC_{50} of TMEM16A is >10-fold larger for Ba^{2+} than for Ca^{2+} (Xiao et al. 2011). The gating of TMEM16A is also permeation ion-dependent. Ca^{2+} sufficiently activates the TMEM16A Cl^- current (Chen et al. 2010), while the Ca^{2+}/CaM complex is indispensable in the HCO_3^- permeation of TMEM16A (Jung et al. 2013). These studies are important for both an understanding of the specificity of physiological regulators of the channel as well as an understanding of the mechanism of channel activation.

In this study, we show that Ca^{2+} can activate stably transfected TMEM16A channels in a voltage-dependent way. The EC_{50} for Ca^{2+} activation is ~300 nM at +80 mV. High intracellular Ca^{2+} concentrations have been reported to eliminate the outward rectification of native

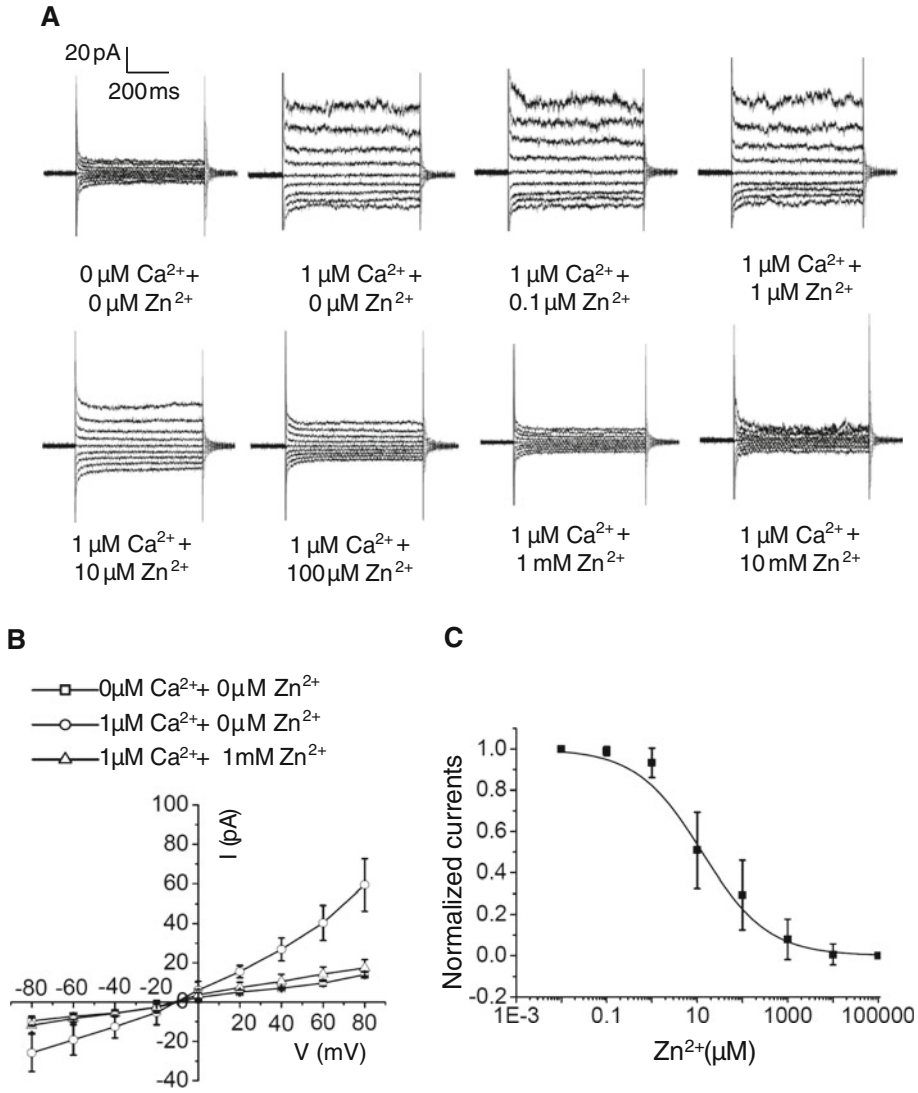

Fig. 7 Zn^{2+} blocks TMEM16A Ca^{2+}-activated currents. **a** Representative current families elicited by 1 μM Ca^{2+} in the presence of increasing concentrations of Zn^{2+} (0–10 mM) applied to the intracellular surface of inside-out membrane patches. Current families were recorded at step potentials from −80 to +80 mV in +20-mV increments from a holding potential of 0 mV. **b** Current–voltage relationships for 0 and 10 μM Ca^{2+} in the presence of the indicated concentration of Zn^{2+} (0 or 1 mM). **c** A concentration–response relationship for block of Ca^{2+}-activated (1 μM Ca^{2+}) TMEM16A currents by intracellular Zn^{2+}. Current magnitudes were normalized to those measured at 1 μM Ca^{2+}, 0 Zn^{2+} at +80 mV in each patch. Data points were fitted to the Hill equation with n_H (slope) = 0.6 and IC_{50} = 12.85 ± 0.28 μM. *Error bars*, mean ± SEM, $n = 7$

CaCCs (Schroeder et al. 2008), yet we did not observe a linearized I–V relationship for TMEM16A currents activated by Ca^{2+}, Sr^{2+} or Ni^{2+} (Figs. 1a,2c, d,3b,4b). One explanation for this is that our recordings from inside-out membrane patches lack a Ca^{2+}-dependent regulator that functions normally to reduce the outwardly rectifying behavior of the channels. In agreement with this suggestion, Xiao et al. (2011) reported that outward rectification of TMEM16A persisted in inside-out patches perfused internally with 25 μM Ca^{2+}. We also found that Sr^{2+} or Ni^{2+} can activate the TMEM16A currents. In both cases, the EC_{50} for channel activation was 30-fold higher than the activation by Ca^{2+}. However, at concentrations of Sr^{2+} or Ni^{2+} that produce saturating effects on TMEM16A current activation, additional activation by Ca^{2+} ions is occluded. The same nonadditivity was measured with Ca^{2+} as the initial activator; at saturating concentrations of Ca^{2+}, the addition of Sr^{2+} and Ni^{2+} produced no greater effect on current activation. Together, these results suggest that the mechanism and site of action of these three divalent cations are common or shared.

Although this has not been well characterized among Ca^{2+}-activated channels, some of them are activated by substitute divalent cations. For example, Ca^{2+}, Cd^{2+} and Sr^{2+} can activate large-conductance Ca^{2+}-activated K^+ (BK) channels by binding at different Ca^{2+} binding sites. Sr^{2+} and Ca^{2+} regulate the BK channel through a Ca^{2+}-bowl mechanism, while Ca^{2+}, Cd^{2+} and Sr^{2+} activate the BK channel by binding at the acidic residues D362/D367 (Zeng et al. 2005). Moreover, besides Ca^{2+}, TMEM16B also can be activated by Sr^{2+} and Ba^{2+}ions (Stephan et al. 2009). Thus, there is a precedent for this phenomenon and the possibility that the electrostatic interactions among divalent cations and negatively charged residues is a shared property of a number of different calcium-activated channels.

Zinc ions have differential effects on ion channels that are regulated by Ca^{2+} and other divalent cations. For example, the TRPA1 (transient receptor potential channel A1) and the BK channel are each activated by intracellular Zn^{2+} (Andersson et al. 2009; Hou et al. 2010), and the ATP-sensitive K^+ channel (K_{ATP}) can be activated by both intracellular and extracellular Zn^{2+} (Prost et al. 2004). However, extracellular Zn^{2+} is reported to block native CaCCs in *Xenopus* oocytes with an IC_{50} of 5.9 μM (Kanjhan and Bellingham 2011). We found that Zn^{2+} (IC_{50} ~13 μM) blocked the Ca^{2+}-activated TMEM16A currents that we stably expressed in HEK cells.

Since the crystal structure of TMEM16A has not been obtained, the precise structural basis of divalent cation regulation of CaCCs is largely unknown. There are some published reports on the structural basis of Ca^{2+} sensitivity of TMEM16A. It has been demonstrated that the previously putative fourth extracellular loop in topological structure of TMEM16A resides on the intracellular side and may contain a Ca^{2+} binding site (Scudieri et al. 2013; Yu et al. 2012). For the putative pore region of TMEM16F, there exist critical amino acid residues that are important for the cation versus anion selectivity of TMEM16F-SCAN (a small-conductance Ca^{2+}-activated nonselective cation) and TMEM16A-CaCC channels (Yang et al. 2012). Xiao et al. (2011) showed that deletion of four amino acids, EAVK (residues 448–451), in the first intracellular loop decreases the apparent affinity for Ca^{2+}-dependent regulation of the channel. Future mechanistic studies will rely on information about the relative affinity of different divalent cations for activation or block of TMEM16A channels. Thus, ours is the first study to characterize the intracellular effects of several divalent cations on TMEM16A channels expressed stably in HEK293T cells. The divalent selectivity sequence for activation was determined to be $Ca^{2+} > Sr^{2+} = Ni^{2+}$. The divalent cations Mg^{2+} and Zn^{2+} failed to activate the TMEM16A channels, but Zn^{2+} blocked the Ca^{2+}-activated currents.

Acknowledgments This work was supported by 11247010 from NSFC and C2012202079 from Hebei NSFC to H. A., 11175055 from NSFC to Y. Z., 31270882 from NSFC and 2013CB531302 from National Basic Research Program to H. Z., and 30900267 from NSFC to Z. Z.

References

Andersson DA, Gentry C, Moss S, Bevan S (2009) Clioquinol and pyrithione activate TRPA1 by increasing intracellular Zn^{2+}. Proc Natl Acad Sci USA 106(20):8374–8379

Bader CR, Bertrand D, Schwartz EA (1982) Voltage-activated and calcium-activated currents studied in solitary rod inner segments from the salamander retina. J Physiol 331:253

Barish ME (1983) A transient calcium-dependent chloride current in the immature *Xenopus* oocyte. J Physiol 342:309–325

Caputo A, Caci ELF, Pedemonte N, Barsanti C, Sondo E et al (2008) TMEM16A, a membrane protein associated with calcium-dependent chloride channel activity. Science 322(5901):590–594

Cenedese V, Betto G, Celsi F, Cherian OL, Pifferi S, Menini A (2012) The voltage dependence of the TMEM16B/anoctamin2 calcium-activated chloride channel is modified by mutations in the first putative intracellular loop. J Gen Physiol 139(4):285–294

Chao SH, Suzuki Y, Zysk JR, Cheung WY (1984) Activation of calmodulin by various metal cations as a function of ionic radius. Mol Pharmacol 26(1):75–82

Chen Y, An H, Li T, Liu Y, Gao C, Guo P, Zhan Y (2010) Direct or indirect regulation of calcium-activated chloride channel by calcium. J Membr Biol 240(3):121–129

Falke JJ, Drake SK, Hazard AL, Peerson OB (1994) Molecular tuning of ion binding to calcium signaling proteins. Q Rev Biophys 27(3):219–290

Ferrera L, Caputo A, Ubby I, Bussani E, Zegarra-Moran O, Ravazzolo R et al (2009) Regulation of TMEM16A chloride channel properties by alternative splicing. J Biol Chem 284(48):33360–33368

Hartzell C, Putzier I, Arreola J (2005) Calcium-activated chloride channels. Annu Rev Physiol 67:719–758

Hou S, Vigeland LE, Zhang G, Xu R, Li M, Heinemann SH, Hoshi T (2010) Zn^{2+} activates large conductance Ca^{2+}-activated K^+ channel via an intracellular domain. J Biol Chem 285(9):6434–6442

Huang F, Rock JR, Harfe BD, Cheng T, Huang X, Jan YN, Jan LY (2009) Studies on expression and function of the TMEM16A calcium-activated chloride channel. Proc Natl Acad Sci USA 106(50):21413–21418

Huang F, Wong X, Jan LY (2012) International Union of Basic and Clinical Pharmacology. LXXXV: calcium-activated chloride channels. Pharmacol Rev 64(1):1–15

Jia Q, Jia Z, Zhao Z, Liu B, Liang H, Zhang H (2007) Activation of epidermal growth factor receptor inhibits KCNQ2/3 current through two distinct pathways: membrane PtdIns(4,5)P2 hydrolysis and channel phosphorylation. J Neurosci 27(10):2503–2512

Jung J, Nam JH, Park HW, Oh U, Yoon JH, Lee MG (2013) Dynamic modulation of ANO1/TMEM16A HCO_3^- permeability by Ca^{2+}/calmodulin. Proc Natl Acad Sci USA 110(1):360–365

Kanjhan R, Bellingham MC (2011) Penetratin peptide potentiates endogenous calcium-activated chloride currents in *Xenopus* oocytes. J Membr Biol 241(1):21–29

MacLeish PR, Nurse CA (2007) Ion channel compartments in photoreceptors: evidence from salamander rods with intact and ablated terminals. J Neurophysiol 98(1):86–95

Miledi R (1982) A calcium-dependent transient outward current in *Xenopus laevis* oocytes. Proc R Soc Lond B 215(1201):491–497

Namkung W, Thiagarajah JR, Phuan PW, Verkman AS (2010) Inhibition of Ca^{2+}-activated Cl^- channels by gallotannins as a possible molecular basis for health benefits of red wine and green tea. FASEB J 24(11):4178–4186

Prost AL, Bloc A, Hussy N, Derand R, Vivaudou M (2004) Zinc is both an intracellular and extracellular regulator of KATP channel function. J Physiol 559(Pt 1):157–167

Schroeder BC, Cheng T, Jan YN, Jan LY (2008) Expression cloning of TMEM16A as a calcium-activated chloride channel subunit. Cell 134(6):1019–1029

Scudieri P, Sondo E, Caci E, Ravazzolo R, Galietta LJ (2013) TMEM16A–TMEM16B chimaeras to investigate the structure–function relationship of calcium-activated chloride channels. Biochem J 452(3):443–455

Stephan AB, Shum EY, Hirsh S, Cygnar KD, Reisert J, Zhao HQ (2009) ANO2 is the cilial calcium-activated chloride channel

that may mediate olfactory amplification. Proc Natl Acad Sci USA 106(28):11776–11781

Xiao QH, Yu K, Perez-Cornejo P, Cui YY, Arreola J, Hartzell HC (2011) Voltage- and calcium-dependent gating of TMEM16A/Ano1 chloride channels are physically coupled by the first intracellular loop. Proc Natl Acad Sci USA 108(21):8891–8896

Yang H, Kim A, David T, Palmer D, Jin T, Tien J et al (2012) TMEM16F forms a Ca^{2+}-activated cation channel required for lipid scrambling in platelets during blood coagulation. Cell 151(1):111–122

Young DY, Cho HW, Koo JY, Tak MH, Cho YY, Shim WS et al (2008) TMEM16A confers receptor-activated calcium-dependent chloride conductance. Nature 455(7217):1210–1236

Yu K, Duran C, Qu Z, Cui YY, Hartzell HC (2012) Explaining calcium-dependent gating of anoctamin-1 chloride channels requires a revised topology. Circ Res 110(7):990–999

Zeng XH, Xia XM, Lingle CJ (2005) Divalent cation sensitivity of BK channel activation supports the existence of three distinct binding sites. J Gen Physiol 125(3):273–286